Green Chemistry

PAPER

View Article Online
View Journal | View Issue

Cite this: *Green Chem.*, 2019, **21**, 4388

Altered carbon assimilation and cellulose accessibility to maximize bioethanol yield under low-cost biomass processing in corn brittle stalk†

Leiming Wu, ‡[a,b] Shengqiu Feng,‡[a,b] Jun Deng,[a,b] Bin Yu,[a,c] Youmei Wang,[a,b] Boyang He,[a,b] Hao Peng,[a,b] Qian Li,[a,b] Ruofei Hu*[d] and Liangcai Peng*[a,b]

Received 15th April 2019,
Accepted 1st July 2019

DOI: 10.1039/c9gc01237k

rsc.li/greenchem

Although cellulosic ethanol has been regarded as an ideal additive for transportation fuels, its low accessibility from recalcitrant lignocellulose renders the bioethanol process unacceptably expensive for commercial production. Here, this study collected the brittle stalk of a corn mutant, *bk1*, that showed similar biomass and seed yields to its wild type (elite cultivar). We then detected significantly reduced cellulose content and degree of polymerization of β-1,4-glucans, leading to a 74% increase in directly-fermentable hexoses accumulation in the brittle stalk by reducing sucrose production and altering carbon assimilation. Notably, under two green-like pretreatments (20 min liquid hot water, 15% CaO at 50 °C), the brittle stalk exhibited remarkably improved cellulose accessibility for almost complete biomass saccharification. This resulted in achieving the highest bioethanol yield of 19.3% (% dry matter) to date, outperforming previous efforts that relied on harsh corn stalk pretreatments. Furthermore, even without any pretreatment, we evaluated that the brittle stalk could deliver a bioethanol yield of 20.3% if the total xylose and hexoses from the brittle stalk were combined for yeast co-fermentation. This study has thus provided a prospective new model for the green-like bioethanol industry that integrates engineered bioenergy crops and yeast strains with cost-effective biomass processing.

1. Introduction

Cellulosic ethanol has been considered a promising solution for the partial replacement of fossil fuels and reduced net carbon release.[1–3] Although lignocellulose represents the most renewable biomass resource, there are three major factors that render bioethanol production unacceptably costly: the intrinsic recalcitrance of lignocellulose, the extrinsic need for planting and collection of bioenergy crops, and potential secondary pollution by wastes and byproducts.[4] Hence, it has become vital to explore an integrated strategy for a cost-effective and green-like biomass process with dedicated bioenergy crops.[5]

The recalcitrance of lignocellulose is mainly caused by its diverse cell wall compositions, specialized wall polymer features and complicated wall-network configurations.[6–9] To reduce recalcitrance, genetic modification of plant cell walls has been implemented in bioenergy crops. In particular, cellulose is directly targeted to increase its accessibility by reducing the degree of polymerization (DP) of β-1,4-glucans and the crystalline index (CrI) of lignocellulose.[10–12] Importantly, although cellulose is the major wall polymer of all biomass resources, its mild modification has only a slight impact on plant growth and biomass or grain yield, indicating a feasible approach for cell wall modification in bioenergy crops.

Furthermore, various chemical pretreatments have been employed to overcome lignocellulose recalcitrance for sequentially enhancing enzymatic saccharification.[13,14] However, most pretreatments lead to a costly biomass process with persistent waste and byproduct formation.[15] In contrast, CaO is a low-cost alkali chemical, but it requires recycling in another industry.[16] Meanwhile, liquid hot water (LHW) is a green-like pretreatment that has been found to cause greatly enhanced enzymatic saccharification in many biomass residues.[17] Therefore, combined one-time genetic lignocellulose modification with green-like pretreatment may lead to a cost-effective biomass process for bioethanol production.

[a]*Biomass and Bioenergy Research Centre, Huazhong Agricultural University, Wuhan, China. E-mail: lpeng@mail.hzau.edu.cn; Fax: +86-27-87280016; Tel: +86-27-87281765, http://bbrc.hzau.edu.cn*
[b]*College of Plant Science and Technology, Huazhong Agricultural University, Wuhan, China*
[c]*Wuhan UniqueGene Bioinformatics Science and Technology Co., Ltd, Wuhan, China*
[d]*College of Food Science and Technology, Hubei University of Arts and Science, Xiangyang 441053, China. E-mail: rhuvip@163.com*

†Electronic supplementary information (ESI) available. See DOI: 10.1039/c9gc01237k

‡Equal contributors.

Plant photosynthesis is the characteristic process that enables the capture of carbon for the storage of solar energy in the form of lignocellulose, starch and soluble sugars in plants. In most plants, sucrose metabolism plays a key role in carbon assimilation from sources (soluble sugars) to sinks (starch, cellulose, others).[18,19] Unlike lignocellulose-based bioenergy crops, sugar- and starch-derived bioenergy crops have been commercially employed for bioethanol production, but their large-scale consumption faces a conflict with food and feed security.[4,20]

Among the widely cultivated food crops worldwide, corn is a highly photosynthetic-efficient C4 plant that annually produces billions of tons of grain and lignocellulose residue.[21] However, except for corn grain, its lignocellulose residue is rarely employed for commercial bioethanol production. In this study, we selected a brittle-stalk mutant (*bk1*) of corn containing much higher levels of soluble sugars and reduced cellulose. We found that this delivered the highest bioethanol yield to date by yeast co-fermentation with the soluble sugars and hexoses released from enzymatic hydrolysis under two green-like pretreatments (CaO, LHW) of the brittle stalk, outperforming previous efforts to obtain cellulosic ethanol under strong pretreatment conditions. Notably, this study also obtained a high bioethanol yield even without any pretreatment of the brittle stalk. Based on analysis of the carbohydrate metabolism, this study presents a hypothetical model that highlights the potential of cost-effective and green-like biomass processing to maximize bioethanol yield in the brittle stalk of corn by altering the carbon flux.

2. Materials and methods

2.1. Collection of brittle stalk in *bk1* mutant

The brittle stalk mutant (single recessive gene, termed *bk1*) was selected from the F_2 seeds of Z31 (wild type/WT, an inbred Chinese maize) crossed with *MuDR* transposon *W22*::*Mu*. The homozygous seeds of WT and *bk1* were obtained by self-fertilization and their stalk samples were regularly collected in the experimental fields of Huazhong Agricultural University, Wuhan from 2013 to 2017. The 11th-leaf stalk was subjected to manual bending for brittle phenotype observation and the mature stalks (without leaves, seeds and roots) were dried, ground through a 40 mesh screen and stored in a dry container for cell wall composition analysis and biomass enzymatic hydrolysis.

2.2. Scanning electron microscopic observation

The top internodes of the corn stalks at the 11th-leaf stage were collected and preserved in formalin-acetic acid-alcohol solution. The plant cell walls were observed using scanning electron microscopy (SEM JSM-5610/LV, Hitachi, Tokyo, Japan). The pretreated biomass residues were dried at 50 °C, and imaged using SEM. Each sample was observed 8–10 times in this study.

2.3. Wall polymers extraction and assay

The cell wall fractionation was conducted as previously described by Peng *et al.*,[22] Jia *et al.*[8] and Li *et al.*[11] The well-mixed biomass powders were initially ground with potassium phosphate buffer (pH 7.0), followed with chloroform–methanol (1 : 1, v/v), DMSO–water (9 : 1, v/v) and 0.5% (w/v) ammonium oxalate to remove lipid, starch and pectin. The residue was extracted with 4 M KOH containing 1.0 mg mL^{-1} sodium borohydride, yielding KOH-extractable hemicelluloses, followed by H_2SO_4 (67%, v/v) to completely dissolve cellulose and non-KOH-extractable hemicelluloses. Cellulose content was calculated by determining the hexoses of the cellulose fraction using the anthrone/H_2SO_4 method.[23] Total hemicelluloses were calculated by determining the hexoses and pentoses using the orcinol/HCl method.[24] Lignin content was measured by the two-step acid hydrolysis method according to the NREL's laboratory analytical protocol (LAP).[25] All experimental analyses were performed in biological triplicate.

2.4. Soluble sugars analysis

The biomass sample (0.300 g) was added into 6 mL distilled water and shaken at 150 rpm for 2 h at 50 °C. After centrifugation at 3000*g* for 5 min, the supernatant was collected for soluble sugar analysis. The pentoses and hexoses of soluble sugars were respectively detected as described above, whereas the fructose, glucose and sucrose were measured using high performance liquid chromatography (HPLC, SHIMADZU, LC-20A with RID-10A detector).

2.5. Fourier transform infrared spectroscopy scanning

A PerkinElmer spectrophotometer (NEXUS 470, Thermo Fisher Scientific, Waltham, MA, USA) was used to qualitatively monitor the biomass samples and the FTIR spectra were recorded in absorption mode over 32 scans at a resolution of 4 cm^{-1} in the range of 4000 to 400 cm^{-1}.

2.6. Cellulose DP and CrI detection

The cellulose degree of polymerization (DP) and crystalline index (CrI) were respectively detected as previously described by Li *et al.*[11] and Hu *et al.*[17] The cellulose DP detection was performed using the crude cellulose samples extracted with 4 M KOH (containing sodium borohydride at 1.0 mg mL^{-1}) and 8% (w/v) $NaClO_2$. All experiments were conducted in triplicate. The X-ray diffraction method was performed to detect the cellulose CrI using a Rigaku D/MAX instrument (Ultima III, Japan). Technical standard errors of the CrI method were measured as ±0.05–0.15 using five representative samples in triplicate.

2.7. Lignocellulose accessibility detection

The cellulose accessibility was estimated by performing Congo red (CR) staining as previously described by Wiman *et al.*[26] with minor modification. The biomass samples (100 mg) were treated with dye solution at a series of concentrations (0.25, 0.50, 1.0, 2.0, 3.0, 4.0 mg mL^{-1}) in 0.3 M phosphate buffer

(pH 6) with 1.4 mM NaCl, and incubated at 60 °C for 24 h. After centrifugation at 8000*g*, the absorbance of the supernatant was measured at 498 nm and the maximum amount of adsorbed dye was calculated by subtraction of free dye in the supernatant from the initial added dye. All measurements were conducted in biological triplicate.

2.8. Hemicellulose monosaccharide and lignin monomer determination

The monosaccharide composition of hemicellulose was determined by GC-MS (SHIMADZU GCMSQP2010 Plus) as previously described by Xu *et al.*[6] and Li *et al.*[10] The lignin monomers were examined by HPLC (LC-20A, SHIMADZU) as previously described by Li *et al.*[11] and Jia *et al.*[8] The standard chemicals *p*-hydroxybenzaldehyde (H), vanillin (G) and syringaldehyde (S) were purchased from Sinopharm Chemical Reagent Co., Ltd.

2.9. Transcriptome sequencing and metabolic pathway analyses

The transcriptome sequencing and metabolic pathway analyses were conducted as previously described by Wang *et al.*[27] The 3rd leaf vein of the corn plant at the 11-leaf stage was flash frozen in liquid nitrogen. Total RNA was isolated using Trizol reagent. The sequencing library for each sample was constructed using the NEBNext mRNA Library Prep Master Mix Set for Illumina (E6110; New England Biolabs) and the NEBNext Multiplex Oligos for Illumina (E7500; New England Biolabs). Paired-end sequencing was performed on an Illumina HiSeq 2500 (Illumina). Genes with fold change ≥2.0 and significance level $p \leq 0.05$ were considered to be differentially expressed. Differentially expressed genes (DEGs) were annotated against the GO and KEGG databases (http://www.genome.jp/kegg/) for function annotation; category enrichment was performed using Blast2GO, with the FDR value of 0.05 in Fisher's exact test, or p value ≤0.05 in the Student's *t*-test. Each sample (mutant, wild type) was analyzed in biological triplicate.

2.10. Biomass pretreatment and enzymatic hydrolysis

Three biomass pretreatments and sequential enzymatic hydrolysis were performed as previously described by Jia *et al.*,[8] Hu *et al.*[17] and Li *et al.*[28] with modification of chemical concentration and incubation time. Acid pretreatment: the well-mixed biomass powder (0.300 g) was added to 6 mL H_2SO_4 at different concentrations (0.5%, 1%, 4%, 6%, v/v) at 5% solid loading, and heated at 121 °C for 20 min in an autoclave (0.15 MPa). Liquid hot water (LHW) pretreatment: the well-mixed biomass powder (0.300 g) was added into well-sealed stainless steel capsules (1 : 8, w/v) at 12.5% solid loading, and heated at 200 °C under 15 rpm shaking for 5, 10, 20, 25 min, respectively. Alkali pretreatment: the biomass power (0.300 g) was added to 6 mL CaO at different concentrations (5%, 10%, 15%, 20%, w/w) with 5% solid loading, and incubated at 50 °C under shaking at 150 rpm for 48 h. Control (without pretreatment): the well-mixed powder was added to 6 mL distilled water at 5% solid loading and shaken at 150 rpm for 2 h at 50 °C.

The pretreated biomass residues were washed once with 10 mL of mixed-cellulase reaction buffer. The washed residues were incubated with 6 mL (2 g L^{-1}) of mixed cellulases (containing cellulases at 10.60 FPU g^{-1} biomass and xylanase at 6.72 U g^{-1} biomass from Imperial Jade Bio-technology Co., Ltd) containing 1% Tween-80 at 5% solid loading, and shaken under 150 rpm for 48 h at 50 °C. The samples were centrifuged at 3000*g* for 5 min, and the supernatants were collected for hexoses and pentose assay. All experiments were carried out in biological triplicate.

2.11. Yeast fermentation and ethanol measurement

Yeast fermentation and ethanol measurement were conducted as previously described by Li *et al.*[11] and Hu *et al.*[17] Yeast of the *Saccharomyces cerevisiae* strain (purchased from Angel Yeast Co., Ltd, Yichang, China) was suspended with 0.2 M phosphate buffer (pH 4.8) for 30 min for activation prior to use. The yeast powder was then added to the phosphate buffer to achieve a final concentration of 0.5 g L^{-1} in all fermentation tubes, and the fermentation was conducted at 37 °C for 48 h in the tubes. Ethanol was measured using the $K_2Cr_2O_7$ method. The experiments were performed in biological triplicate.

3. Results and discussion

3.1. Reduced cellulose and increased soluble sugars in the *bk1* mutant

Using mutator-inserted technology, this study selected a genetically stable brittle-stalk mutant (*bk1*) of corn by crossing elite inbred corn Z31 (wild type/WT, an elite Chinese cultivar) with *MuDR* transposon (*W22*::*Mu*). Compared with the WT, the homozygous *bk1* mutant consistently exhibited normal growth with only slightly affected biomass and grain yields in three-season field experiments (Fig. 1A and Fig. S1†), which was similar to our previously identified rice brittle-culm mutant showing normal growth and high biomass and grain yields.[10] However, as the *bk1* mutant was of a brittle-stalk phenotype under manual bending, we observed thinner sclerenchyma cell walls under SEM (Fig. 1B and C). With respect to the thinner cell walls of the brittle stalk, the *bk1* mutant contained significantly lower cellulose levels than that of the WT at $p < 0.01$ ($n = 3$), with a relative cellulose reduction of 29%, but the mutant and WT did not show significantly different hemicelluloses and lignin levels at $p > 0.05$ (Fig. 1D). In addition, this study found that the *bk1* mutant and WT were similar with respect to both the monosaccharide composition of hemicellulose and the monomer composition of lignin (Tables S1 and S2†), suggesting that the thinner cell walls of the brittle stalk were mainly due to its reduced cellulose level, rather than the non-cellulosic polymers in the *bk1* mutant. Notably, unlike the rice brittle-culm mutant, the *bk1* mutant contained much higher levels of soluble sugars than those of the WT, with a 65%

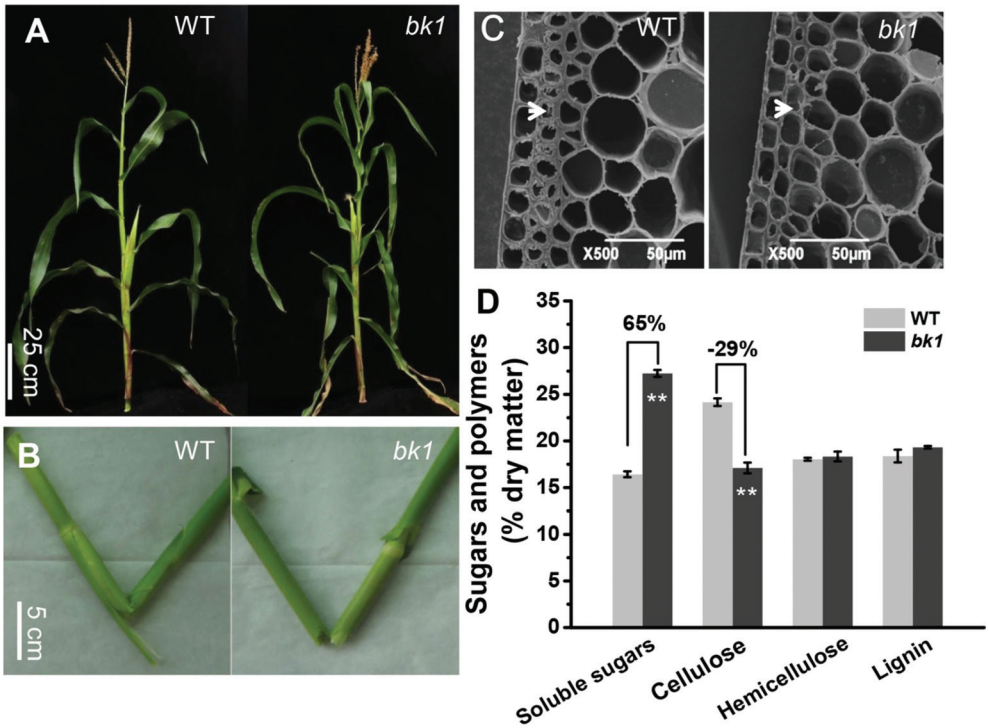

Fig. 1 Characterization of corn *bk1* mutant. (A) The *bk1* mutant and its wild type (WT) showing normal plant growth. (B) A brittle-stalk phenotype in the *bk1* mutant under manual bending. (C) Relatively thin cell walls observed in the brittle stalk of *bk1* mutant under SEM. (D) Increased soluble sugars and reduced cellulose contents (% dry matter) in the *bk1* mutant. **As significant differences between the *bk1* and WT by Student's *t*-test at $p < 0.01$ ($n = 3$) with the increased/decreased (–) percentage of the *bk1* mutant relative to the WT, and data as means ± SD ($n = 3$).

increase in the brittle stalk (Fig. 1D). Among the total soluble sugars that were increased in the *bk1* mutant, we further found that the hexose and pentose levels were increased by 74% and 25% (Fig. 2A), respectively, indicating that significantly altered carbon flux may occur in the *bk1* mutant. Because sucrose is the end product of plant photosynthesis,[29] the brittle stalk of the *bk1* mutant contained a reduced sucrose level by 15% with increased fructose and glucose by 6% and 20% (Fig. 2B), respectively, suggesting that altered sucrose metabolism may dynamically regulate carbon partitioning and allocation in the brittle stalk of the *bk1* mutant.

3.2. Enhanced hexoses and ethanol yields in brittle stalk under three pretreatments

Using our previously established approach,[8,11,12,17] this study examined biomass enzymatic saccharification of the brittle stalk by measuring hexose yields (% cellulose) released from enzymatic hydrolyses under three distinct biomass pretreat-

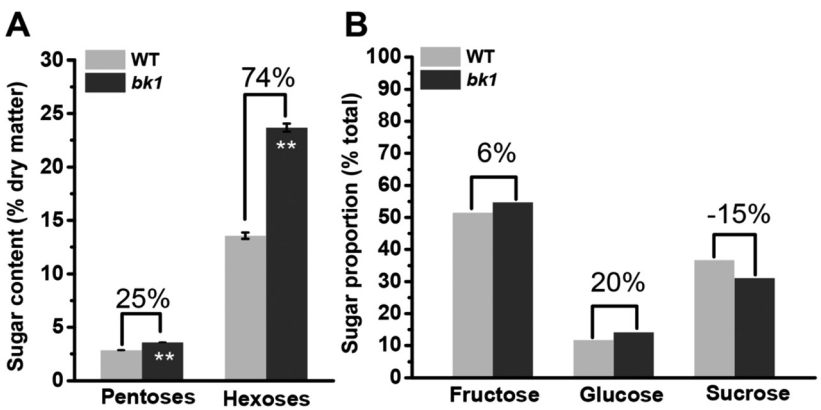

Fig. 2 Soluble sugar composition of the brittle stalk in the *bk1* mutant. (A) The *bk1* mutant containing significantly increased hexoses and pentoses relative to the WT. (B) The *bk1* mutant containing relatively high fructose and glucose and low sucrose. **As significant differences between the *bk1* and WT by Student's *t*-test at $p < 0.01$ ($n = 3$) with the increased percentage of the *bk1* mutant relative to WT, and data as means ± SD ($n = 3$).

ments (Fig. 3A–C). In comparison, the *bk1* mutant consistently exhibited much higher hexose yields than those of the WT either from the acid pretreatment with various H_2SO_4 concentrations (0.5%, 1%, 4%, 6%) or from the LHW pretreatment over a range of times (5, 10, 20, 25 min). In particular, the 20 min LHW treatment led to an almost complete biomass enzymatic saccharification with a hexose yield of 96% in the brittle stalk. In addition, under 5% and 10% CaO pretreatments, the *bk1* mutant showed significantly higher hexose yields than those of the WT, but pretreatment with saturated CaO (15%) achieved a hexose yield of 100% in both mutant and WT.

Consequently, this study performed a classic yeast fermentation for bioethanol production using total soluble sugars and hexoses released from enzymatic hydrolysis under the three optimal pretreatments (Fig. 3D–G). Compared to the WT and the control (without pretreatment), the *bk1* mutant exhibited significantly higher ethanol yields with the rates increased by 10% to 37% at the $p < 0.05$ or 0.01 level ($n = 3$) under the three optimal pretreatments, consistent with its higher levels of soluble sugars and hexose yields as described above. In particular, the *bk1* mutant had a higher ethanol yield of 19.3% (% dry matter) under the two optimal green-like pretreatments (20 min LHW, 15% CaO), compared to the previously reported ethanol yields (16.2%, 13.0%) obtained from corn stalk processing, despite the harsh pretreatment conditions in the previous cases (Table 1).[30–32] Although ammonia fiber expansion pretreatment of corn stover led to the ethanol yield of 19.1%, this was due to a yeast co-fermentation of hexoses and xylose.[33] Assuming that all xyloses obtained from soluble sugars and hemicellulose hydrolysis were co-fermented by the engineered yeast strain in the brittle stalk, from the results of the present study it was roughly estimated that the *bk1* mutant could respectively achieve the ethanol yields of 24.3% under the two optimal green-like pretreatments, based on the average xylose-ethanol conversion rate as previously reported (Table 1). Hence, the data revealed that combining the green-like LHW pretreatment with the brittle stalk mutation could achieve much higher bioethanol production without any secondary chemical waste release to the environment. Notably, without any pretreatment, the brittle stalk still achieved a high bioethanol yield of 15.2%, even rising to 20.3% if adding

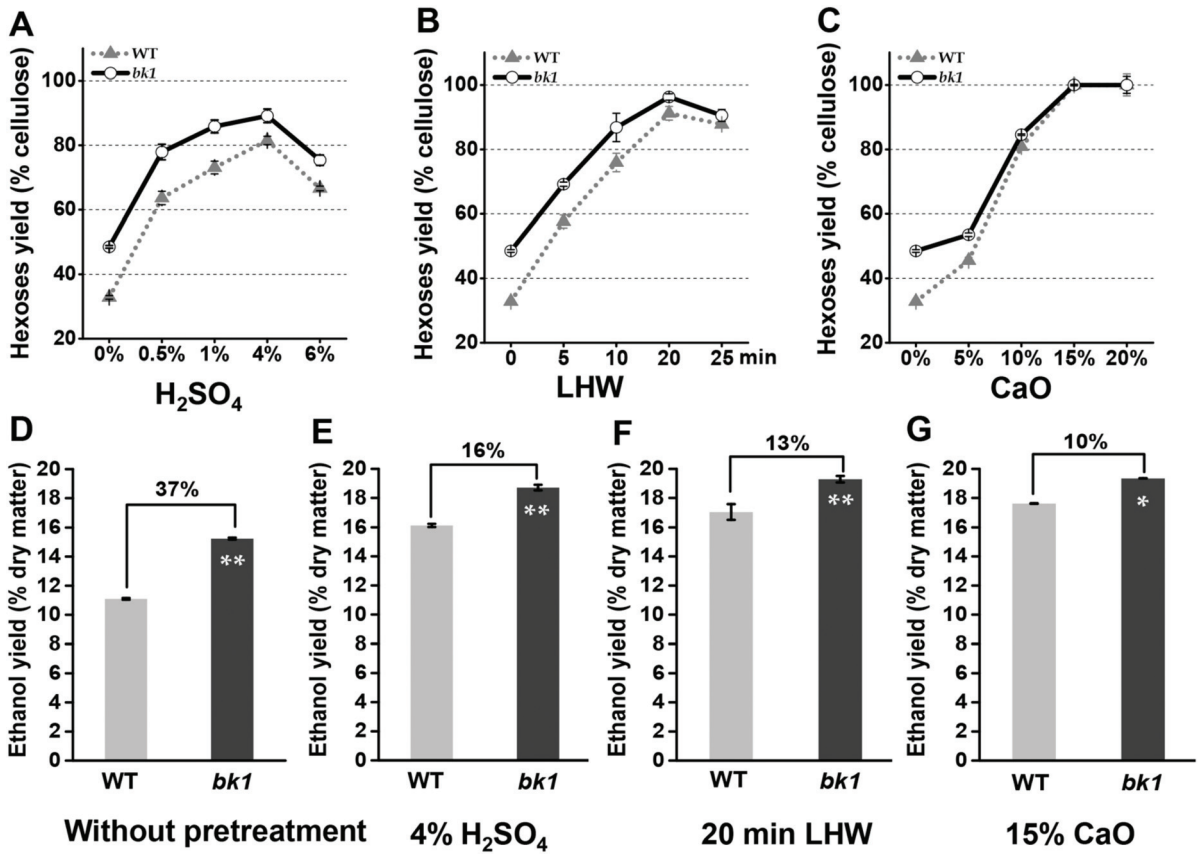

Fig. 3 Enhanced biomass saccharification and bioethanol production of the brittle stalk in the *bk1* mutant. (A), (B) and (C) Hexoses yields (% cellulose) released from enzymatic hydrolysis under acid (H_2SO_4, A), liquid hot water (LHW, B) and alkali (CaO, C) pretreatments. (D), (E), (F) and (G) Bioethanol yields (% dry matter) obtained from yeast fermentation using soluble sugars and hexoses released from enzymatic hydrolysis under three optimal pretreatments (D, control/without pretreatment; E, 4% H_2SO_4; F, 20 min LHW; G, 15% CaO). * and **As significant differences between the *bk1* and WT by Student's *t*-test at $p < 0.05$ and 0.01 ($n = 3$) with the increased percentage of the *bk1* mutant relative to the WT, and data as means ± SD ($n = 3$).

Table 1 Bioethanol yields (% dry matter) obtained in the *bk1* mutant and other corn samples under different pretreatments

Pretreatment	Hexoses fermentation only	Hexoses & pentoses co-fermentation	Solid loading for enzymatic hydrolysis	Ref.
Without pretreatment	15.24%	20.28%[c]	5%	This study
4% H_2SO_4	18.71%	23.75%	5%	
20 min LHW	19.29%	24.33%	5%	
15% CaO	19.35%	24.39%	5%	
AFEX[a]		19.15%	17.6%	33
MBSP[b]	16.15%		10%	30
1% H_2SO_4 + steam explosion	12.99%		10%	31
Ionic liquid	7.22%		6%	32

[a] Ammonia fiber expansion. [b] Magnesium bisulfite pretreatment. [c] Based on the average xylose-ethanol conversation rate of 35% as previously reported by Rodrussamee *et al.* (2018)[53] and Valinhas *et al.* (2018).[54]

all xyloses into the yeast co-fermentation (Table 1), providing a cost-effective bioethanol production technology without any chemical processing. This was mainly due to increased soluble sugars (hexoses, pentoses) accumulation and higher hexoses yield released by direct enzymatic hydrolysis in the brittle stalk, but it may also be subjected to less inhibitor formation from the direct enzymatic hydrolysis of the brittle stalk, favouring efficient sugar-ethanol conversion during yeast fermentation.[15,34] In addition, this study only performed low solid loading experiments, and thus it remains to determine the optimal green-like technology for bioethanol production at high concentration (g L^{-1}) with increased solid loading of corn brittle stalk, along with high dosages of the cellulase enzyme supplement and engineered yeast strain for xylose and hexoses co-fermentation in the future.

3.3. Decreased cellulose DP and improved biomass accessibility in the brittle stalk

To understand why the *bk1* mutant achieved greatly enhanced biomass enzymatic saccharification for bioethanol production, this study detected the cellulose DP values of stalks in both mutant and WT (Fig. 4). In general, the *bk1* mutant was found to have significantly lower cellulose DP values than those of the WT at the $p < 0.01$ level ($n = 3$) in all raw stalk materials (without pretreatment) and the three optimally pretreated biomass residues (Fig. 4A). In particular, all pretreated biomass residues also had much lower cellulose DP values than those of the raw stalk materials in both mutant and WT. Because it has been well characterized that cellulose DP negatively affects lignocellulose enzymatic hydrolysis in various biomass residues,[11,12] the reduction of cellulose DP values in the *bk1* mutant should be a major factor accounting for its increased biomass enzymatic saccharification. Similarly, the *bk1* mutant was also detected to have consistently reduced lignocellulose CrI values in all samples, but the pretreated residues had higher lignocellulose CrI values than those of the raw stalk materials (Fig. S2†), which is probably due to partial wall polymer extraction during the pretreatments.[35] Hence, although lignocellulose CrI is a negative factor for biomass enzymatic hydrolysis,[6,7,10] its reduction probably only makes a minor contribution to the increased enzymatic saccharification of the pretreated biomass residues in both *bk1* mutant and WT relative to their raw stalk materials.

As cellulose accessibility is a direct parameter affecting biomass enzymatic hydrolysis, this study further performed Congo red staining on all biomass samples, which has been widely used to measure the specific surface area of cellulose.[26,35] Significantly, the *bk1* mutant exhibited much larger Congo red staining areas than those of the WT in all samples examined, in particular for the three pretreated biomass residues, which had increased staining areas by 22% to 34% (Fig. 4B), indicating a remarkably improved cellulose accessibility leading to high biomass enzymatic saccharification in the brittle stalk of the *bk1* mutant. Furthermore, correlation analysis has been widely applied to account for the effects of wall polymer features on biomass enzymatic saccharification in various lignocellulose samples.[36–38] Therefore, this study performed a similar analysis and found that cellulose DP values were negatively correlated with hexoses yields at the $p < 0.01$ level ($n = 24$), whereas cellulose accessibility had a significantly positive correlation with hexose yield, with a high R value of 0.887 (Fig. 4C and D), which confirmed that the greatly enhanced biomass saccharification of the brittle stalk was mainly due to its significantly reduced cellulose DP and increased accessibility under the three optimal pretreatments. In addition, this study found that cellulose DP values were negatively correlated with cellulose accessibility (Fig. S3†), consistent with the previously proposed assumption that the reduced cellulose DP should reflect increased amorphous regions of cellulose microfibrils, enabling more cellulase enzyme access and loading during lignocellulose hydrolysis.[11,12]

3.4. Unaltered wall polymer extraction in brittle stalk after pretreatments

With regard to the *bk1* mutant having only slightly altered hemicellulose and lignin levels in the brittle stalk, this study also examined wall polymer extraction upon the optimal three pretreatments and estimated the overall mass balances among the three optimal pretreatments, subsequent enzymatic hydrolysis, and final yeast fermentation (Fig. 5 and Fig. S6–S8†). Both the *bk1* mutant and WT yielded a major hemicellulose extraction from 4% H_2SO_4 pretreatment or 20 min LHW pretreatment, while a predominant removal of lignin was obtained from 15% CaO pretreatment with little cellulose extraction (Table S3†). Using Fourier transform infrared spectroscopy, we observed that the pretreated biomass residues exhibited characteristic alteration of the peaks in both the *bk1* mutant and WT compared to their controls without pretreatment (Fig. 6).[39,40] For example, the peaks at 1727 cm^{-1} were

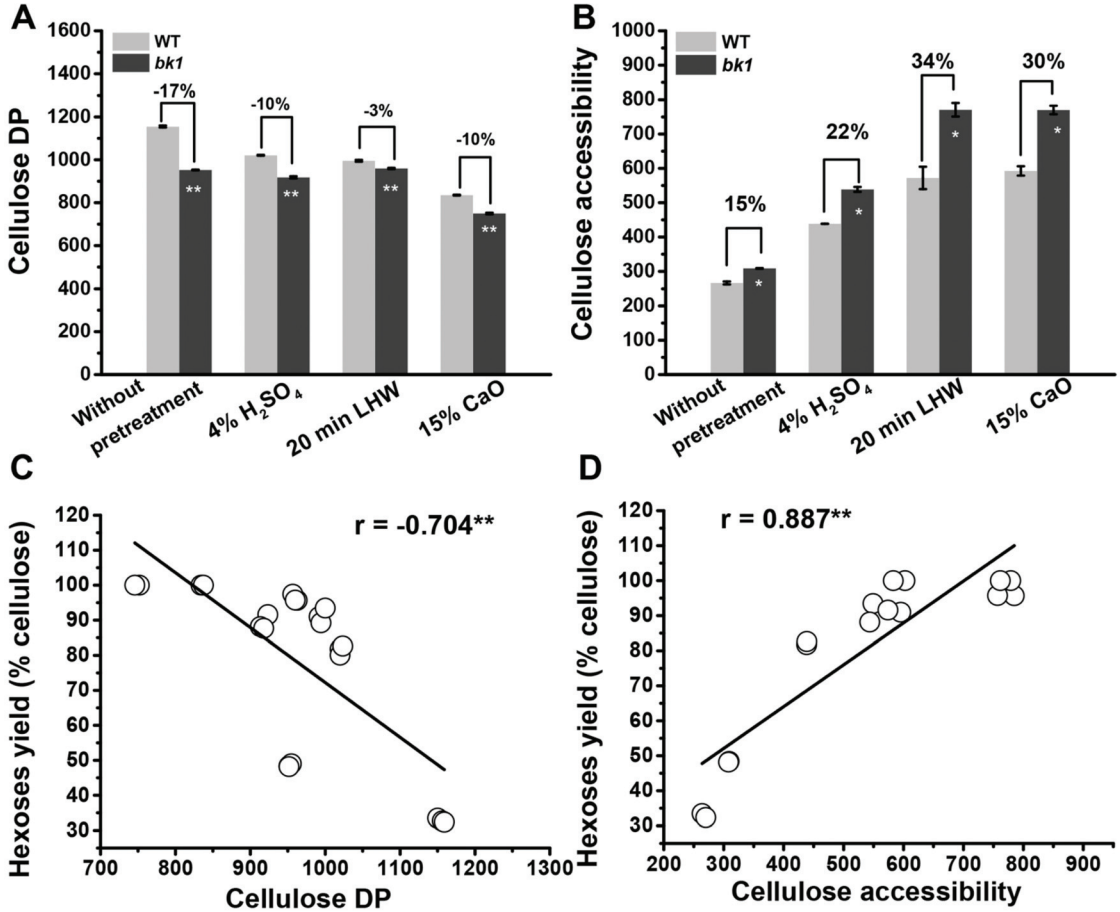

Fig. 4 Impacts of cellulose DP and accessibility on biomass enzymatic saccharification. (A) and (B) Significantly reduced cellulose DP (A) and raised cellulose accessibility (B) in the raw stalk material and three optimally pretreated biomass residues of *bk1* mutant. Cellulose accessibility (B) defined by Congo red stain area ($m^2\ g^{-1}$). * and **As significant differences between the *bk1* and WT by Student's *t*-test at $p < 0.05$ and 0.01 ($n = 3$) with the increased/decreased (–) percentage of the *bk1* mutant relative to the WT, and data as means ± SD ($n = 3$). (C) and (D) Correlation analysis between the cellulose DP ($n = 22$) (C) or accessibility ($n = 16$) (D) and hexoses yields released from enzymatic hydrolysis under three optimal pretreatments and control (without pretreatment). **As significant correlation at $p < 0.01$.

almost absent in all three optimally pretreated residues of the mutant and WT. These peaks are assigned to (C═O) bonds in either ester-linked acetyl and uronic groups of the hemicelluloses or carboxylic acid groups of ferulic and *p*-coumaric acids of lignin and hemicelluloses (Table S4†), suggesting an almost complete removal of hemicellulose-lignin linkages by the three optimal pretreatments.[41] The absorption peaks at 1247 cm^{-1} showed much reduced intensities, particularly in the LHW pretreated residues. These peaks are assigned to the (C–O–C) aryl–alkyl ether bonds in lignin.[42] However, we did not observe much difference in the characteristic peaks of the *bk1* mutant and WT in the pretreated biomass residues relative to their raw stalks. In addition, the *bk1* mutant and WT did not display greatly different topology of the pretreated biomass residues under SEM (Fig. S4†). Taken together, these data indicate that the *bk1* mutant predominantly underwent changes to its cellulose features (DP, accessibility) in its raw stalk material and pretreated biomass residues but little alteration of non-cellulosic polymers (hemicellulose, lignin) compared to the WT.

3.5. Altered sucrose metabolism pathway and carbon flux

To understand why the *bk1* mutant displayed reduced cellulose content and increased soluble sugar in its brittle stalk, we performed a transcriptomic analysis to observe differentially expressed genes (DEGs) between the *bk1* mutant and WT (Fig. S5A†). As a result, approximately 387 down-regulated and 312 up-regulated genes were sorted out among a total of 46 430 genes identified in the *bk1* mutant (Fig. S5B†). Based on the enrichment annotation of the DEGs, most DEGs were found to be involved in sucrose metabolism, carbohydrate transport, cellulose biosynthesis, cell wall formation and other related biological processes (Fig. S5C†). By profiling sucrose synthesis and the related carbohydrate metabolism (Fig. 7 and Table S5†), several representative genes, including the sucrose synthase (SUS) gene, were identified to regulate the sucrose synthetic pathway, resulting in reduced sucrose and UDP-glucose products, leading to increasing soluble sugar (hexoses) accumulation in the brittle stalk of the *bk1* mutant (Fig. 7A

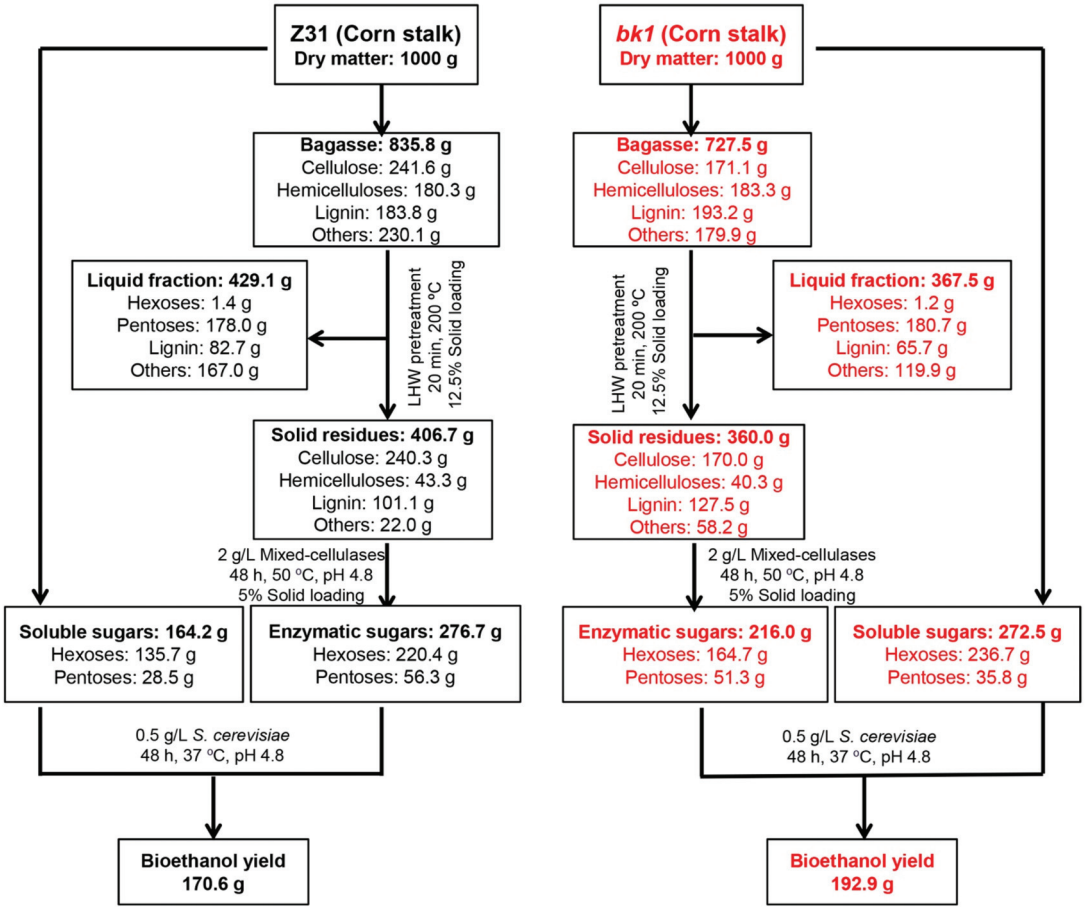

Fig. 5 Mass balance for lignocellulose conversion to ethanol between Z31 (WT, left) and *bk1* (mutant, right) under 20 min LHW pretreatment.

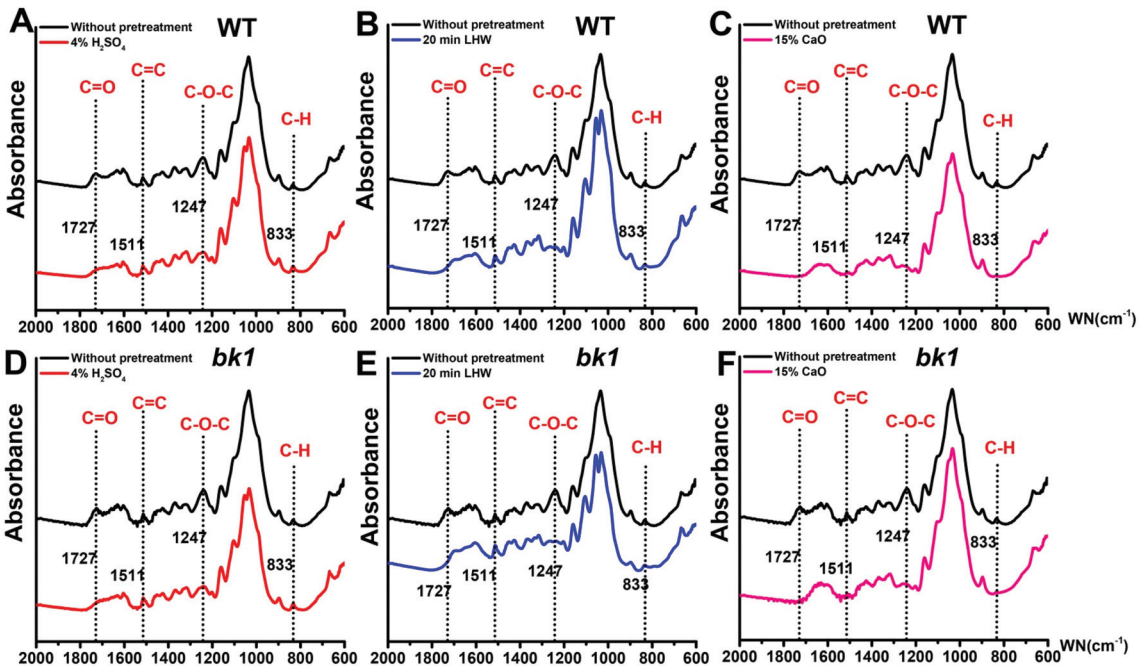

Fig. 6 Fourier transform infrared spectroscopic profiling of raw stalk materials (without pretreatment) and pretreated biomass residues. (A), (B) and (C) WT samples. (D), (E) and (F) *bk1* samples. The characteristic peaks are assigned in ESI Table 4.†

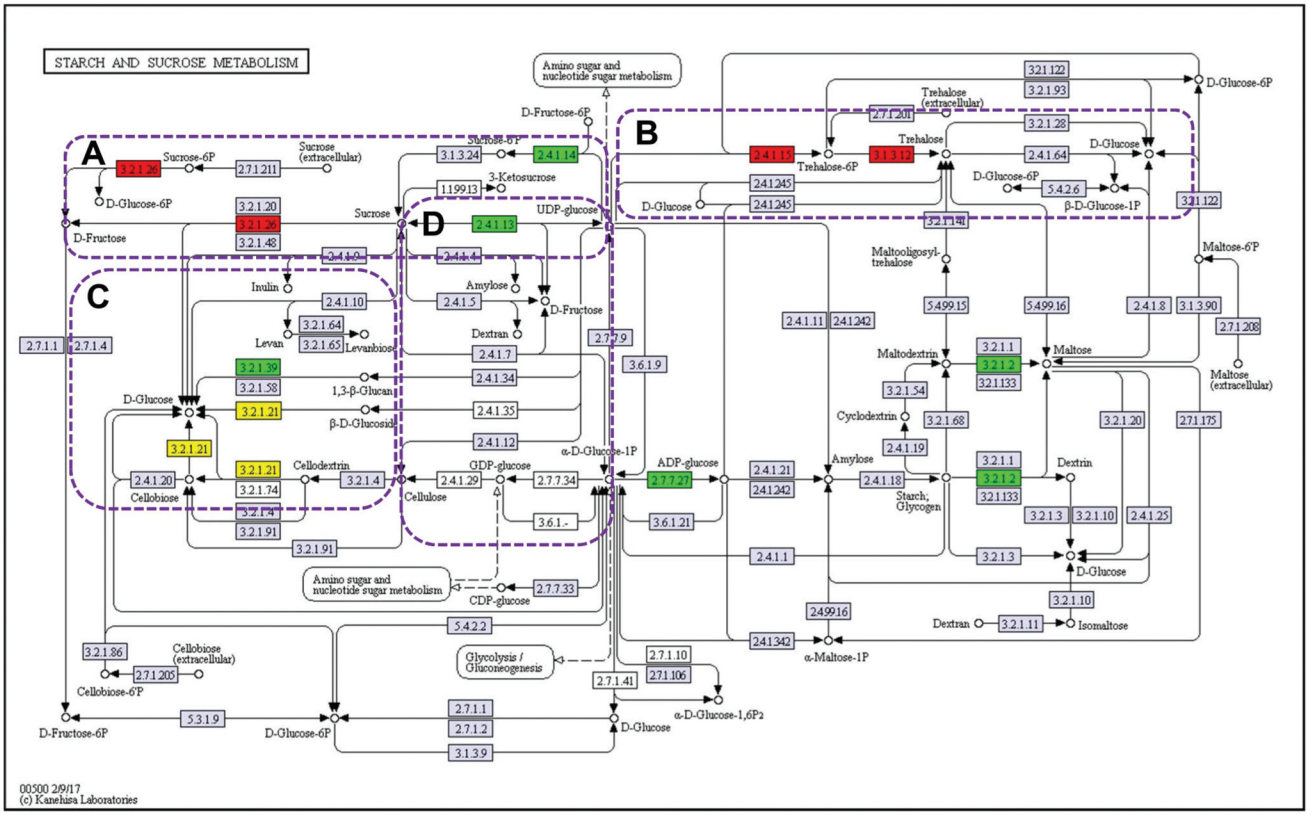

Fig. 7 Alteration of sucrose and carbohydrate metabolism pathways in the *bk1* mutant. (A) Down-regulated sucrose synthesis. (B) and (C) Increased glucose allocation and accumulation. (D) Down-regulated cellulose synthesis. Red boxes highlight up-regulated genes/enzymes; green boxes are down-regulated genes; yellow boxes are dual up/down-regulated genes; grey and white boxes are insignificantly altered genes. The representative genes/enzymes are listed in ESI Table 5.†

and B). Since UDP-glucose is the unique substrate for cellulose biosynthesis,[43–45] the reduced amount of this substrate should directly affect cellulose production in the brittle stalk (Fig. 7D). Furthermore, because it has been recently characterized that overproduction of β-glucosidases can lead to reduced cellulose DP and CrI in transgenic rice,[11,12] the up-regulated β-glucosidase may play a similar role in the reduction of the cellulose features (DP, CrI) herein, possibly leading to soluble glucose accumulation in the brittle stalk (Fig. 7C). Therefore, the transcriptomic analysis shed some light on why the brittle stalk of the *bk1* mutant contained significantly reduced cellulose levels and DP with increased soluble sugar allocation.

While genetic modification of plant cell walls has been implemented by targeting non-cellulosic polymers (hemicellulose, lignin, pectin) for reducing lignocellulose recalcitrance in various bioenergy crops,[5,46–52] it has more recently been reported that slight cellulose alteration can lead to a direct improvement of cellulose accessibility in genetic mutant and transgenic plants with little impact on plant growth and biomass/grain yield.[10–12] Although our preliminary results indicated that the *bk1* mutant is mutated in the candidate gene with a characteristic defect of sucrose synthesis, this study also identified several important genes involved in carbon flux regulation and improvement of cellulose features as described above. Therefore, those genes could be combined with the mutant candidate gene for comprehensive genetic engineering of bioenergy corn and other crops using advanced synthetic biological approaches in the near future, which may allow more precise integrative enhancements of both soluble sugar allocation and lignocellulose enzymatic digestibility in bioenergy crops.

3.6. A hypothetical model for low-cost and green-like bioethanol production

Taking all the data together, we propose a hypothetical model that highlights the cost-effective and green-like biomass process enabling maximum ethanol production in the brittle stalk of a corn mutant, based on the following evidence (Fig. 8): (1) With respect to the starch-rich grain/seeds of corn potent for food/feed or bioethanol production, utilization of its lignocellulose could save planting costs compared to dedicated bioenergy crops (switchgrass, *Miscanthus*, *etc.*); (2) Due to the reduced cellulose level and improved accessibility of the brittle stalk, the green-like LHW pretreatment was sufficient for complete lignocellulose enzymatic hydrolysis, which suggested the possibility of directly using solar energy for greener LHW pretreatment; (3) Using soluble sugars and

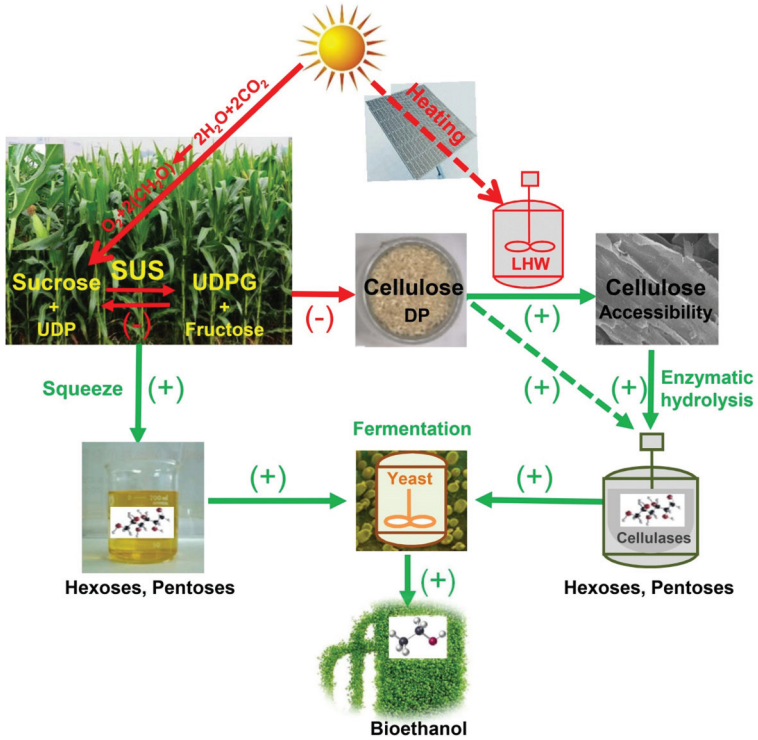

Fig. 8 A hypothetical model to highlight a green-like strategy for the bioethanol industry by integrating engineered bioenergy crops and yeast strains with low-cost biomass processing. The engineered bioenergy crop should be of significantly improved cellulose accessibility for an efficient enzymatic saccharification with very high soluble sugars accumulation for direct ethanol fermentation. The engineered yeast strain should be able to use both hexoses and pentose (xylose) as carbon sources for co-fermentation. (–) and (+) respectively are reducing and enhancing strategies for biomass processing and bioethanol production in the model; "SUS" is sucrose synthase.

hexoses released from direct enzymatic hydrolysis of the brittle stalk without any pretreatment, this study still achieved high bioethanol yield, and the remaining pure cellulose residue could be applied as a value-added material for other industries, indicating a potential technology for very low-cost and benefit-added biomass processing without any chemical waste release. However, it remains to identify the key factors/parameters accounting for green-like bioethanol production in the corn brittle stalk and other bioenergy crops in the future.[55] Therefore, this study provided a powerful strategy for the green-like bioethanol industry by combining engineered bioenergy crops and yeast strains with low-cost (LHW or no pretreatment) biomass processing.

4. Conclusions

Using the brittle stalk of the corn *bk1* mutant, showing significantly reduced cellulose content and DP with remarkably increased soluble sugars, this study demonstrated an almost complete biomass enzymatic saccharification, achieving the highest-yet bioethanol yield of 19.3% (% dry matter) under two green-like pretreatments optimized to greatly enhance the cellulose accessibility. Furthermore, even without any chemical pretreatment, the brittle stalk could provide an ethanol yield of 20.3% if total xylose and hexoses from soluble sugars and direct lignocellulose enzymatic hydrolysis were combined for yeast co-fermentation. Therefore, this study has revealed a hypothetical model of green-like bioethanol production that combines desirable bioenergy crops and engineered yeast strains with low-cost biomass processing by dynamically altering carbon assimilation for highly fermentable sugar accumulation in the crop stalk.

Conflicts of interest

The authors have no conflicts of interest to declare.

Acknowledgements

This work was in part supported by grants from the National Natural Science Foundation of China (31670296; 31571721; 31200911), the Project of Huazhong Agricultural University Independent Scientific & Technological Innovation Foundation (2014bs04), the National Key Research and Development Program (2016YFD0800804), the National 111 Project (B08032) and the Project of Hubei University of Arts and Science (XKQ2018006).

References

1 A. Carroll and C. Somerville, *Annu. Rev. Plant Biol.*, 2009, **60**, 165.
2 D. W. Wakerley, M. F. Kuehnel, K. L. Orchard, K. H. Ly, T. E. Rosser and E. Reisner, *Nat. Energy*, 2017, **2**, 17021.
3 E. M. Rubin, *Nature*, 2008, **454**, 841–845.
4 G. S. Xie and L. C. Peng, *J. Integr. Plant Biol.*, 2011, **53**, 143–150.
5 Y. T. Wang, C. F. Fan, H. Z. Hu, Y. Li, D. Sun, Y. M. Wang and L. C. Peng, *Biotechnol. Adv.*, 2016, **34**, 997–1017.
6 N. Xu, W. Zhang, S. F. Ren, F. Liu, C. Q. Zhao, H. F. Liao, Z. D. Xu, J. F. Huang, Q. Li, Y. Y. Tu, B. Yu, Y. T. Wang, J. X. Jiang, J. P. Qin and L. C. Peng, *Biotechnol. Biofuels*, 2012, **5**, 58.
7 W. Zhang, Z. L. Yi, J. F. Huang, F. C. Li, B. Hao, M. Li, S. F. Hong, Y. Z. Lv, W. Sun, A. Ragauskas, F. Hu, J. H. Peng and L. C. Peng, *Bioresour. Technol.*, 2013, **130**, 30–37.
8 J. Jia, B. Yu, L. M. Wu, H. W. Wang, Z. L. Wu, M. Li, P. Y. Huang, S. Q. Feng, P. Chen, Y. L. Zheng and L. C. Peng, *PLoS One*, 2014, **9**, e108449.
9 F. C. Li, M. L. Zhang, K. Guo, Z. Hu, R. Zhang, Y. Q. Feng, X. Y. Yi, W. H. Zou, L. Q. Wang, C. Y. Wu, J. S. Tian, T. G. Lu, G. S. Xie and L. C. Peng, *Plant Biotechnol. J.*, 2015, **13**, 514–525.
10 F. C. Li, G. S. Xie, J. F. Huang, R. Zhang, Y. Li, M. L. Zhang, Y. T. Wang, A. Li, X. K. Li, T. Xia, C. C. Qu, F. Hu, A. J. Ragauskas and L. C. Peng, *Plant Biotechnol. J.*, 2017, **15**, 1093–1104.
11 Y. Li, P. Liu, J. F. Huang, R. Zhang, Z. Hu, S. Q. Feng, Y. T. Wang, L. Q. Wang, T. Xia and L. C. Peng, *Green Chem.*, 2018, **20**, 2047–2056.
12 J. F. Huang, T. Xia, G. H. Li, X. L. Li, Y. Li, Y. T. Wang, Y. M. Wang, Y. Y. Chen, G. S. Xie, F. W. Bai, L. C. Peng and L. Q. Wang, *Biotechnol. Biofuels*, 2019, **12**, 11.
13 K. Karimi and M. J. Taherzadeh, *Bioresour. Technol.*, 2016, **200**, 1008–1018.
14 Y. Lan, H. Yang, G. Chang, Y. Pu, X. Meng, W. Muchero, G. Tuskan, T. Tschaplinski and A. Ragauskas, *Bioresour. Technol.*, 2018, **265**, 75.
15 L. Jönsson and C. Martín, *Bioresour. Technol.*, 2015, **199**, 103–112.
16 J. Xu, J. J. Cheng, R. Sharma-Shivappa and J. Burns, *Bioresour. Technol.*, 2010, **101**, 2900–2903.
17 M. Hu, H. Yu, Y. Li, A. Li, Q. M. Cai, P. Liu, Y. Y. Tu, Y. T. Wang, R. F. Hu, B. Hao, L. C. Peng and T. Xia, *Carbohydr. Polym.*, 2018, **202**, 434–443.
18 Y. L. Ruan, *Annu. Rev. Plant Biol.*, 2014, **65**, 33–67.
19 D. P. Delmer and C. H. Haigler, *Metab. Eng.*, 2002, **4**, 22–28.
20 S. T. Yang, H. A. Elenshasy and N. Thongchul, *Green Process. Synth.*, 2013, **2**, 637–637.
21 Z. Yan, A. Damgaard and T. H. Christensen, *Prog. Energy Combust.*, 2018, **67**, 275–291.
22 L. C. Peng, C. H. Hocart, J. W. Redmond and R. E. Williamson, *Planta*, 2000, **211**, 406–414.
23 S. C. Fry, *The growing plant cell wall: chemical and metabolic analysis*, Longman, London, 1988.
24 Z. Dische, C. Pallavicini, H. Kavasaki, N. Smirnow, L. J. Cizek and S. Chien, *Arch. Biochem. Biophys.*, 1962, **97**, 459–469.
25 Z. Zhang, I. M. O'Hara and W. O. Doherty, *Bioresour. Technol.*, 2012, **120**, 149–156.
26 M. Wiman, D. Dienes, M. A. Hansen, T. V. Meulen, G. Zacchi and G. Lidén, *Bioresour. Technol.*, 2012, **126**, 208–215.
27 Y. F. Wang, A. Q. Zheng, F. L. Sun, M. Li, K. J. Xu, C. Zhang;, S. D. Liu and Y. J. Xi, *Front. Plant Sci.*, 2018, **9**, 1805.
28 M. Li, S. Q. Feng, L. M. Wu, Y. Li, C. F. Fan, R. Zhang, W. H. Zou, Y. Y. Tu, H. C. Jing, S. Z. Li and L. C. Peng, *Bioresour. Technol.*, 2014, **167**, 14–23.
29 T. D. Sharkey, M. Stitt, D. Heineke, R. Gerhardt, K. Raschke and H. W. Heldt, *Plant Physiol.*, 1986, **81**, 1123–1129.
30 H. Yu, J. Ren, L. Lei, Z. Zheng, J. Zhu, Y. Qiang and O. Jia, *Bioresour. Technol.*, 2016, **199**, 188–193.
31 J. Zhu, Y. Rong, J. Yang, X. Zhou, Y. Xu, L. Zhang, J. Chen, Q. Yong and S. Yu, *Appl. Biochem. Biotechnol.*, 2015, **176**, 1370–1381.
32 G. Papa, S. Rodriguez, A. George, A. Schievano, V. Orzi, K. L. Sale, S. Singh, F. Adani and B. A. Simmons, *Bioresour. Technol.*, 2015, **183**, 101–110.
33 M. W. Lau and B. E. Dale, *Proc. Natl. Acad. Sci. U. S. A.*, 2009, **106**, 1368–1373.
34 H. Li and H. Chen, *Process Biochem.*, 2008, **43**, 1447–1451.
35 V. Pihlajaniemi, M. H. Sipponen, H. Liimatainen, J. A. Sirviö, A. Nyyssölä and S. Laakso, *Green Chem.*, 2016, **18**, 1295–1305.
36 Z. L. Wu, M. L. Zhang, L. Q. Wang, Y. Y. Tu, J. Zhang, G. S. Xie, W. H. Zou, F. C. Li, K. Guo, Q. Li, C. B. Gao and L. C. Peng, *Biotechnol. Biofuels*, 2013, **6**, 183–183.
37 Y. J. Pei, Y. Y. Li, Y. B. Zhang, C. B. Yu, T. D. Fu, J. Zou, Y. Y. Tu, L. C. Peng and C. Peng, *Bioresour. Technol.*, 2016, **203**, 325–333.
38 J. F. Huang, Y. Li, Y. T. Wang, Y. Y. Chen, M. Y. Liu, Y. M. Wang, R. Zhang, S. G. Zhou, J. Y. Li, Y. Y. Tu, B. Hao, L. C. Peng and T. Xia, *Biotechnol. Biofuels*, 2017, **10**, 294.
39 Q. Wang, W. Wei, G. P. Kingori and J. Sun, *Cellulose*, 2015, **22**, 3559–3568.
40 A. Rogina, A. Ressler, I. Matić, G. G. Ferrer, I. Marijanović, M. Ivanković and H. Ivanković, *Carbohydr. Polym.*, 2017, **166**, 173–182.
41 D. Jiang, D. F. Zhuang, J. Y. Fu, Y. H. Huang and K. G. Wen, *Renewable Sustainable Energy Rev.*, 2012, **16**, 1377–1382.
42 M. E. Himmel, S. Y. Ding, D. K. Johnson, W. S. Adney, M. R. Nimlos, J. W. Brady and T. D. Foust, *Science*, 2007, **315**, 804–807.
43 C. H. Haigler, M. Ivanova-Datcheva, P. S. Hogan, V. V. Salnikov, S. Hwang, K. Martin and D. P. Delmer, *Plant Mol. Biol.*, 2001, **47**, 29–51.
44 L. C. Peng, K. Yasushi, H. Pat and D. Deborah, *Science*, 2002, **295**, 147–150.

45 C. Somerville, *Annu. Rev. Cell Dev. Biol.*, 2006, **22**, 53–78.
46 K. A. Gray, L. Zhao and M. Emptage, *Curr. Opin. Chem. Biol.*, 2006, **10**, 141–146.
47 J. L. Field, S. G. Evans, E. Marx, M. Easter, P. R. Adler, T. Dinh, B. Willson and K. Paustian, *Nat. Energy*, 2018, **3**, 211–219.
48 C. H. Lee, Q. Teng, W. L. Huang, R. Q. Zhong and Z. H. Ye, *Plant Cell Physiol.*, 2009, **50**, 1075–1089.
49 L. Vincenzo, F. Fedra, F. Simone, V. Chiara, B. Daniela, G. Roberta, D. O. Renato, D. L. Giulia and C. Felice, *Proc. Natl. Acad. Sci. U. S. A.*, 2010, **107**, 616–621.
50 K. W. Zhang, M. W. Bhuiya, J. R. Pazo, Y. C. Miao, H. Kim, J. Ralph and C. J. Liu, *Plant Cell*, 2012, **24**, 3135–3152.
51 V. Ruben, C. Igor, R. Katarzyna, X. Yuguo, S. Lisa, G. Geert, K. Hoon, C. Joanna, M. Kris and A. Pedro, *Science*, 2013, **341**, 1103–1106.
52 L. L. Cheng, L. Q. Wang, L. Y. Wei, Y. Wu, A. Alam, C. B. Xu, Y. T. Wang, Y. Y. Tu, L. C. Peng and T. Xia, *Green Chem.*, 2019, **21**, 3693–3700.
53 N. Rodrussamee, P. Sattayawat and M. Yamada, *BMC Microbiol.*, 2018, **18**, 73.
54 R. V. Valinhas, L. A. Pantoja, A. C. Maia, D. L. Nelson and A. S. Santos, *PeerJ*, 2018, **6**, e4673.
55 A. Alam, R. Zhang, P. Liu, J. F. Huang, Y. T. Wang, Z. Hu, M. Madadi, D. Sun, R. F. Hu, A. J. Ragauskas, Y. Y. Tu and L. C. Peng, *Biotechnol. Biofuels*, 2019, **12**, 99.